MOEM

Modern Electronic Materials 2022; 8(3): 113–121
DOI 10.3897/j.moem.8.3.98758

Research Article

Kinetics of oxygen sorption-desorption processes in manganites of $La_{0.7}Sr_{0.3}Mn_{0.9}Fe_{0.1}O_{3-\delta}$ composition

Alexander L. Gurskii[1], Nikolay A. Kalanda[2], Marta V. Yarmolich[2], Alexander V. Petrov[2], Petr N. Kireev[3], Deleg Sangaa[4], Ping-Zhan Si[5]

1 Belarusian State University of Informatics and Radioelectronics, 6 P. Brovka Str., Minsk 220013, Belarus

2 Scientific-Practical Materials Research Centre of the National Academy of Sciences of Belarus, 19 P. Brovka Str., Minsk 220072, Belarus

3 Powder Metallurgy Institute of the National Academy of Sciences of Belarus, 41 Platonov Str., Minsk 220005, Belarus

4 Institute of Physics and Technology of the Mongolian Academy of Sciences, 54B Peace Ave., Ulaanbaatar 13330, Mongolia

5 China Jiliang University, 258 Xueyuan Str., Hangzhou 310018, China

Corresponding author: Alexander L. Gurskii (algur106@tut.by)

Received 12 September 2022 ♦ **Accepted** 19 September 2022 ♦ **Published** 20 October 2022

Citation: Gurskii AL, Kalanda NA, Yarmolich MV, Petrov AV, Kireev PN, Sangaa D, Si PZh (2022) Kinetics of oxygen sorption-desorption processes in manganites of $La_{0.7}Sr_{0.3}Mn_{0.9}Fe_{0.1}O_{3-\delta}$ composition. *Modern Electronic Materials* 8(3): 113–121. https://doi.org/10.3897/j.moem.8.3.98758

Abstract

Based on the data of thermogravimetric analysis the values of the oxygen index (3–δ) in the manganite of the $La_{0.7}Sr_{0.3}Mn_{0.9}Fe_{0.1}O_{3-\delta}$ composition, obtained by solid-phase reaction technique, have been calculated. The analysis of oxygen sorption-desorption curves showed that the processes of oxygen release and absorption at pO_2 = 10 Pa and pO_2 = 400 Pa are not reversible. The minima of the derivative $d\delta/dt = f(T)$ corresponding to the maxima of the oxygen extraction rate indicate the complex character of changes in the oxygen desorption rate from manganite. The decrease in the heating and cooling rate from 6.6 K/min to 2.6 K/min resulted in a significant change in the value Δδ, indicating the dependence of anion mobility on the oxygen concentration in the magnet structure. It has been revealed that in the $La_{0.7}Sr_{0.3}Mn_{0.9}Fe_{0.1}O_{3-\delta}$ manganite the oxygen desorption kinetics is well described by the exponential dependence on the Kramers model, which implies no return of desorbed oxygen to the sample. This model indicates the non-stationarity of the diffusion flux through the barrier during desorption of oxygen from samples. The calculation of the activation energy of oxygen desorption by the Merzhanov method at various partial pressures of oxygen has shown that at the initial stage of oxygen extraction from $La_{0.7}Sr_{0.3}Mn_{0.9}Fe_{0.1}O_{3-\delta}$, the activation energy of oxygen desorption has a minimum value (E_a = 103.7 kJ/mol at δ = 0.005) and as the concentration of oxygen vacancies increases, it rises reaching saturation (E_a = 134.3 kJ/mol at δ = 0.06). It is assumed that with an increase in the concentration of oxygen vacancies, an interaction occurs between them, followed by the processes of their ordering with the formation of associates.

Keywords

doped manganites, oxygen non-stoichiometry, thermogravimetric analysis, sorption and desorption processes, activation energy

© 2022 National University of Science and Technology MISiS. This is an open access article distributed under the terms of the Creative Commons Attribution License (CC-BY 4.0), which permits unrestricted use, distribution, and reproduction in any medium, provided the original author and source are credited.

1. Introduction

Doped manganites $La_{0.7}Sr_{0.3}Mn_{1-x}Fe_xO_{3-\delta}$ (x = 0–0.15) with different cationic composition are strongly electron-correlated systems, with the presence of competing electron-electron, electron-magnon and electron-phonon interactions [1–3]. This leads to the formation of orbital and charge ordering in such systems, which contributes to the appearance of giant magnetoresistance due to spin-dependent scattering of conduction electrons in the presence of indirect exchange coupling and magnetic anisotropy [4–10]. In this case, spin-polarized transport phenomena, promising from the point of view of practical use in magnetic field sensors, cathode materials, magnetic recording heads, for reliable storage and reading of information, etc., depend on structural inhomogeneities of various types [7–10]. Thus, electrical resistivity is determined by various mechanisms of scattering of electric charge carriers on structural inhomogeneities located both in the grain volume and on its surface. One of the sources of such disorder is the inhomogeneity of the electron density distribution due to the presence of different valence cations $Fe^{2+,3+}$ and $Mn^{3+,4+}$ with various ionic radii [11–14]. It has been established that even small deformations of the unit perovskite cell (that is, an increase in the Mn–O bond length or a decrease in the Mn–O–Mn angle) significantly change the properties of the material [10–16]. Also, structural distortions are oxygen vacancies $V_O^{\bullet}$, as well as their associates $(V_O\ V_O\ \ldots)^{\bullet\bullet n}$ of the n-th order, along which diffusion channels with a reduced activation energy for anionic transport are formed [12–17]. In this case, the charge transfer in $La_{0.7}Sr_{0.3}Mn_{1-x}Fe_xO_{3-\delta}$ is carried out under conditions of various kinds of structural disorder, which leads to the possibility of the presence of quantum interference effects in the low-temperature region. In this case, quantum interference is due to an increase in the probability of electron-electron interaction due to diffusion rather than ballistic motion of charge carriers with multiple elastic scattering on structural inhomogeneities and, above all, on anion vacancies and their associates [11–17]. In this case, it is necessary to take into account the complexity of the processes of sorption and desorption of oxygen by solid solutions $La_{0.7}Sr_{0.3}Mn_{1-x}Fe_xO_{3-\delta}$ due to the multi-stage movement of desorbed oxygen and the low mobility of cations of oxygen vacancies [16–19].

The use of manganites in magnetic and spin electronics requires the employment materials of stoichiometric composition with a stable single-phase state. Obtaining manganites with the required electrical-physical characteristics is associated with great technological difficulties due to the lack of knowledge about the kinetics of oxygen sorption – desorption in these materials [5, 13–18]. Therefore, the investigation of the kinetics of desorption – sorption of oxygen, the establishment of a correlation between the kinetic characteristics of oxygen exchange of $La_{0.7}Sr_{0.3}Mn_{1-x}Fe_xO_{3-\delta}$ with their chemical composition will optimize the functional characteristics of doped lanthanum-strontium manganites. At the same time, obtaining single-phase solid solutions with reproducible physical and chemical properties is impossible without a detailed analysis of the effect of the partial pressure of oxygen on the values of the activation energy of its diffusion in $La_{0.7}Sr_{0.3}Mn_{1-x}Fe_xO_{3-\delta}$ polycrystalline samples. In the ideal structure of manganite, an ordered arrangement of MnO_3 octahedra is observed, with a spatial arrangement of Sr cations occupying voids between the octahedra, which leads to a decrease in the free energy of the lattice.

A further decrease in the free energy of the lattice is due to the presence of anionic defects, which affect the galvanomagnetic characteristics of the manganites as well. Therefore, in order to obtain reproducible physico-chemical properties of manganites, it is necessary, on the basis of studying the kinetics of oxygen sorption and desorption processes, to work out the modes for the synthesis of magnets with a controlled oxygen content.

As an object of study, we have chosen the $La_{0.7}Sr_{0.3}Mn_{0.9}Fe_{0.1}O_{3-\delta}$ compound, in which the partial replacement of Mn cations by Fe makes it possible to more finely set the Curie point and obtain the T_C values required for its practical use.

The purpose of this work is to obtain experimental data on the kinetics of oxygen desorption in the $La_{0.7}Sr_{0.3}Mn_{0.9}Fe_{0.1}O_{3-\delta}$ by thermogravimetric analysis **(TGA)**, analyze them on the basis of known theoretical models, and determine the activation energy of oxygen desorption depending on the oxygen partial pressure.

2. Experimental

La_2O_3, Fe_2O_3, Mn_2O_3 metal oxides and strontium carbonate $SrCO_3$ have been used for the preparation of $La_{0.7}Sr_{0.3}Mn_{0.9}Fe_{0.1}O_{3-\delta}$ solid solutions. To remove crystallization moisture, the initial chemical compounds were kept in a resistive thermal device for 10 h at a temperature of 1120 K. Homogenizing agitation of a mixture of a stoichiometric amount of initial metal oxides and strontium carbonate has been carried out in ethanol. The resulting mixture was dried at a temperature of 370 K until the complete removal of ethanol and pressed into tablets 12 mm in diameter and 5 mm thick.

Mixing and grinding of the mixture of initial reagents of stoichiometric composition was carried out in a planetary ball mill of the PM 100 type by Retsch GmbH (Germany), which makes it possible to obtain a charge grain size of submicron sizes 200–300 nm. Grinding was carried out with steel bodies with different time durations (2–5 h) and in different environments (dry grinding or the process in ethanol). In this case, the vibration frequency of the mill was 1500 min^{-1}, the vibration amplitude was 10 mm, and the weight ratio material/balls corresponded to 1/5. If the grinding procedure was performed in ethanol, then the resulting mixture was dried at a temperature of 320 K until the complete removal of ethanol and

pressed under a pressure of 1–2 T/cm^2 into tablets 8 mm in diameter and 4 mm high.

Annealing of a stoichiometric mixture of simple oxides was carried out in a polythermal mode at temperatures of 300–1400 K at $pO_2 = 0.21 \cdot 10^5$ Pa and a heating rate of 2 deg/min for 15 h. The samples were cooled in the switched-off mode of the thermal set-up. The temperature in the thermal set-ups has been maintained using a RIF-101 temperature controller and monitored using a Pt–Pt/Rh(10%) thermocouple with an accuracy of ±0.5 K.

The phase composition and crystal lattice parameters were determined by the Rietveld method using the ICSD-PDF2 database (Release 2000) and the PowderCell [20], FullProf [21] software based on X-ray diffraction data obtained on a DRON-3 set-up in CuK_α radiation. Diffractograms were taken at room temperature at a rate of 60 deg/h in the range of angles θ = 10–90°.

The investigation of the nature of oxygen desorption by lanthanum-strontium manganite depending on the partial pressure of oxygen was carried out by TGA using the Setaram Labsys TG–DSC16 measuring complex at various heating rates in the range of 300–1300 K. The samples were kept until thermodynamic equilibrium with the gaseous medium has been established, and then cooled to room temperature in a continuous flow of a 1% H_2/Ar gas mixture. The sign of the achievement of thermodynamic equilibrium was the absence of a change in the mass of the sample at a fixed temperature of the samples. The weight of the samples was controlled by weighing with an accuracy of $\pm 3 \cdot 10^{-5}$ g.

3. Results and discussion

Based on the TGA data, the values of the oxygen index (3–δ) were calculated. Time dependences of oxygen nonstoichiometry for samples of the composition $La_{0.7}Sr_{0.3}Mn_{0.9}Fe_{0.1}O_{3-\delta}$, obtained during heating at a rate of 6.6 deg/min, exposure to equilibrium with the gas phase at T = 1300 K and subsequent cooling are shown in Fig. 1.

When studying the $La_{0.7}Sr_{0.3}Mn_{0.9}Fe_{0.1}O_{3-\delta}$ samples, the onset of oxygen evolution was found at 858 K, which continued up to 1273 K. One maximum of the oxygen desorption rate was found at a temperature of 1256 K, when the rate of oxygen evolution was the highest (Fig. 1). It has been established that the processes of oxygen evolution and absorption at pO_2 = 10 Pa, shown in Fig. 1 are not fully reversible. When the samples have been cooled down from a temperature of 1273 K, an insignificant absorption of oxygen was observed with a weakly pronounced maximum of its adsorption rate at a temperature of 1167 K. It should be noted that when the $La_{0.7}Sr_{0.3}Mn_{0.9}Fe_{0.1}O_{3-\delta}$ sample reached a temperature of 1270 K, the manganite was not in thermodynamic equilibrium with a gas environment. At the same time, its oxygen index (3–δ) continued to decrease from 2.952 to 2.916 upon reaching oxygen saturation. Then the thermal set-up was cooled down at the same rate (6.6 deg/min) and at the end of the thermal cycle the oxygen content was 2.921 at 300 K.

Time dependences of oxygen nonstoichiometry for samples of the composition $La_{0.7}Sr_{0.3}Mn_{0.9}Fe_{0.1}O_{3-\delta}$, obtained during heating at pO_2 = 10 Pa at a rate of 2.6 K/min and holding until equilibrium with the gas phase has been established at temperature (1273 K), are shown in Fig. 2.

The decrease in the heating and cooling rate for the $La_{0.7}Sr_{0.3}Mn_{0.9}Fe_{0.1}O_{3-\delta}$ sample is caused by the fact that, as was established above, this sample during annealing was not in thermodynamic equilibrium with the gas medium, which can lead to an incorrect description of the processes of oxygen sorption and desorption. The minima

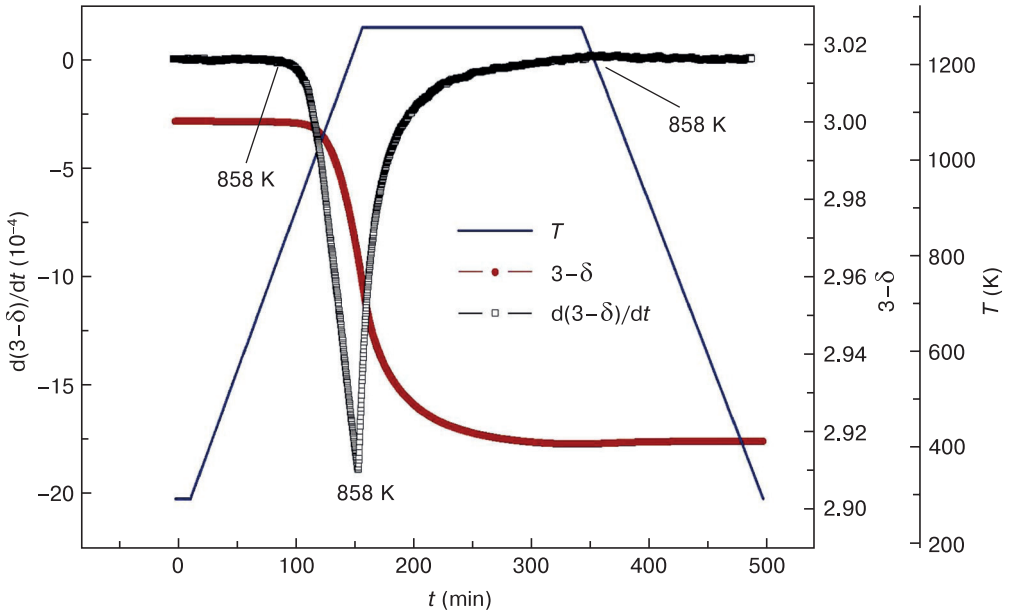

Figure 1. Change in the value of the oxygen index (3–δ) and the derivative dδ/dt=$f(T)$ during thermal cycling of $La_{0.7}Sr_{0.3}Mn_{0.9}Fe_{0.1}O_{3-\delta}$ samples with a heating and cooling rate of 6.6 K/min at pO_2 = 10 Pa

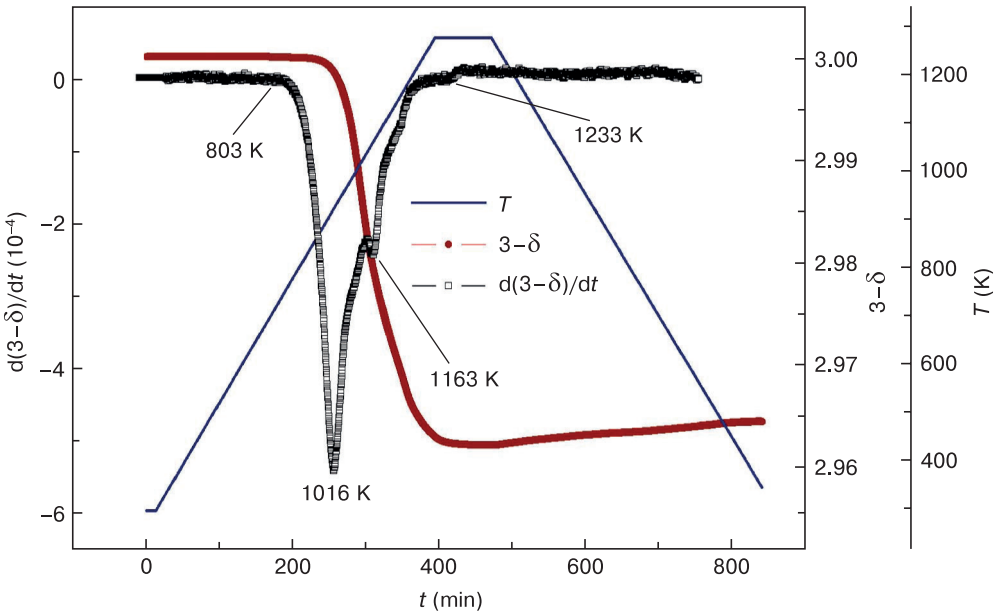

Figure 2. Change in the value of the oxygen index (3–δ) and the derivative d**δ**/dt=$f(T)$ during thermal cycling of $La_{0.7}Sr_{0.3}Mn_{0.9}Fe_{0.1}O_{3-\delta}$ samples with a heating and cooling rate of 2.6 K/min at pO_2 = 400 Pa

of the derivative dδ/dt = $f(T)$, which correspond to the maxima of the rate of oxygen release, indicate the complex nature of the change in the rate of oxygen desorption from manganite. When analyzing the desorption-sorption curves of oxygen by a magnet, a splitting of the oxygen desorption peak with the appearance of two minima has been found: the first one at T = 1016 K and the second one at T = 1163 K. In this case, the release of oxygen during heating begins at a temperature of 803 K and is observed up to 1273 K.

The processes of oxygen evolution and absorption shown in Fig. 2 are not completely reversible, as well. It can be seen that the oxygen content in $La_{0.7}Sr_{0.3}Mn_{0.9}Fe_{0.1}O_{3-\delta}$ at the beginning and at the end of the cycles does not coincide with each other. Based on the TGA data, the values of the oxygen index for the magnet were calculated. For ceramic samples $La_{0.7}Sr_{0.3}Mn_{0.9}Fe_{0.1}O_{3-\delta}$ brought to equilibrium at the maximum annealing temperature of 1273 K, δ = 2.961 (see Fig. 2). Subsequent heating leads to an increase in δ to 2.964 for samples subjected to thermal cycling at pO_2 = 10 Pa.

A decrease in the rate of heating and cooling made it possible to increase the oxygen index, while the process of oxygen sorption is practically absent. This is due to the fact that the mobility of anions depends on the concentration of oxygen in the material, since this process is associated with kinetic difficulties due to different cooling rates.

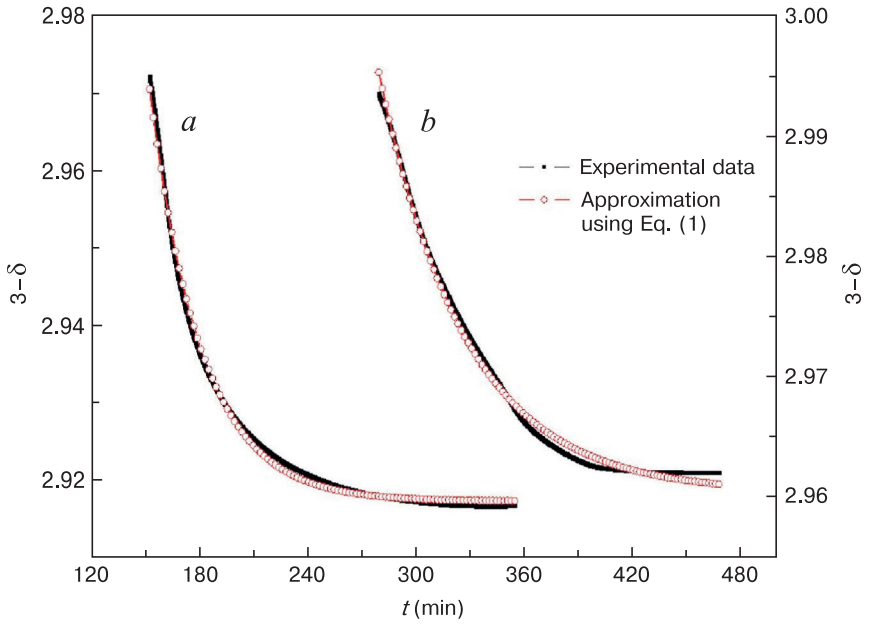

Figure 3. Kinetic dependencies of oxygen desorption of samples $La_{0.7}Sr_{0.3}Mn_{0.9}Fe_{0.1}O_{3-\delta}$ at pO_2 = 10 Pa (*a*) and pO_2 = 400 Pa (*b*)

Thus, when analyzing oxygen sorption–desorption curves, it was found that the processes of oxygen evolution and absorption at pO_2 = 10 Pa and pO_2 = 400 Pa are not reversible. The minima of the derivative $d\delta/dt = f(T)$, which correspond to the maxima of the rate of oxygen release, indicate the complex nature of the change in the rate of oxygen desorption from manganite. A decrease in the heating and cooling rate from 6.6 K/min to 2.6 K/min led to a significant change in the value of $\Delta\delta$ at pO_2 = 400 Pa, which indicates anions on the concentration of oxygen in the structure of the magnet.

When studying the kinetics of oxygen evolution, mathematical models were considered to obtain theoretical dependencies based on experimental data $\delta = f(t)$, received earlier. Note that the desorption rate is noticeably higher than the sorption rate, which is practically absent; therefore, we will not consider it further. Let us consider various models of diffusion and chemical kinetics to describe the kinetic curves of oxygen desorption obtained on the basis of TGA data, which will make it possible to establish the limiting stage of oxygen diffusion and determine the mechanism of oxygen desorption. The kinetic dependences of the oxygen desorption of $La_{0.7}Sr_{0.3}Mn_{0.9}Fe_{0.1}O_{3-\delta}$ samples have reached a plateau at the holding time t_1 = 330 min and t_2 = 420 min, respectively (Fig. 3).

It has been established that in manganites at different pO_2 values, the kinetics of oxygen desorption is best described by the exponential dependence [22–24]:

$$\xi = \xi_0 + A\exp\left(-\frac{t}{\tau}\right), \quad (1)$$

where $\xi = 3 - \delta$, $\xi_0 = 3 - \delta_0$, δ_0 is the value of the oxygen nonstoichiometry coefficient at the initial time of the oxygen desorption process, A is the proportionality factor, τ is the relaxation time. In order to describe the kinetics of oxygen desorption, the Kramers model [22, 23] was used, which implies the absence of the return of desorbed oxygen to the sample. In this case, the probability $W(t - t_0)$ of the absence of oxygen leakage has an exponential form:

$$W(t - t_0) = \exp\left[-w_k(t - t_0)\right], \quad (2)$$

where w_k is the Kramers probability of oxygen exit from the sorption potential well by thermally activated overcoming of the barrier. As the annealing temperature increases, the amplitude of thermal fluctuations increases and the probability of oxygen leaving the sorption energy well increases. The mathematical formalism based on the use of the modified Kramers method indicates the non-stationarity of the diffusion flow through the barrier during oxygen desorption from $La_{0.7}Sr_{0.3}Mn_{0.9}Fe_{0.1}O_{3-\delta}$ samples. In this case, the mobility of oxygen is determined by the interaction of anions with local active centers in the near-surface region, which are Mn/Fe or La/Sr cations. This circumstance affects the values of the relaxation times. It can be assumed that the depth of the sorption well is greater, since the relaxation time τ_{10Pa} = 28.93 ± 0.13 min is less than τ_{400Pa} = 48.40 ± 0.26 min (Table 1). The kinetic parameters calculated according to the Kramers model from diffusion kinetics presented in the table indicate that the oxygen desorption rate decreased down to pO_2 = 400 Pa and, accordingly, the anion mobility decreased. As it can be seen from the data obtained, by means of the change of the oxygen partial pressure we can influence the desorption properties of oxygen in manganites.

The investigation of the effect of oxygen partial pressure on the values of activation energy of its diffusion in polycrystalline samples $La_{0.7}Sr_{0.3}Mn_{0.9}Fe_{0.1}O_{3-\delta}$ as the parameter δ changes was carried out on the basis of TGA data obtained with different heating rates (1, 4, 7, 10 and 13 deg/min) at pO_2 = 400 Pa and pO_2 = 10 Pa in the temperature range 300–1400 K (Fig. 4). The achievement of thermodynamic equilibrium was determined by the absence of a change in the mass of the samples at a fixed temperature of the samples.

When analyzing the temperature dependences of oxygen desorption processes for the $La_{0.7}Sr_{0.3}Mn_{0.9}Fe_{0.1}O_{3-\delta}$ sample, it was found that at all heating rates, the oxygen index does not reach saturation at T = 1400 K. It can be observed in the inset to Fig. 4 shows that a pronounced release of oxygen during heating of the samples at a heating rate of 1 deg/min starts from $T \sim 735$ K, $T \sim 728$ K at pO_2 = 400 Pa and pO_2 = 10 Pa, respectively. With an increase in the heating rate to 13 deg/min, the onset of oxygen evolution shifts towards higher temperatures, reaching values of $T \sim 771$ K, $T \sim 759$ K at pO_2 = 400 Pa and pO_2 = 10 Pa, respectively. When analyzing the amount of desorbed oxygen, an increase in its values with a decrease in the heating rate (v_H) was established: $\Delta\delta = |\delta_{300K} - \delta_{1420K}| = 0.052$ for v_H = 13 deg/min and $\Delta\delta = 0.078$ for v_H = 1 deg/min. This circumstance indicates a significant effect of the heating rate on the values of the activation energy of oxygen diffusion during its evolution.

Currently, there are several models that describe the course of chemical processes in a solid during the synthesis of complex oxides and oxide compounds. The main

Table 1. Kinetic parameters of equation (1) for studied manganites and their coefficients of determination

$La_{0.7}Sr_{0.3}Mn_{0.9}Fe_{0.1}O_{3-\delta}$ at pO_2 = 10 Pa				$La_{0.7}Sr_{0.3}Mn_{0.9}Fe_{0.1}O_{3-\delta}$ at pO_2 = 400 Pa			
ξ_0	A_{10Pa}	τ_{10Pa} (min)	R^2	ξ_0	A_{400Pa}	τ_{400Pa} (min)	R^2
$2.9607 \pm 4.5 \cdot 10^{-4}$	11.1 ± 0.34	28.9 ± 0.13	0.99	$2.9173 \pm 3.6 \cdot 10^{-4}$	9.7 ± 0.24	48.4 ± 0.26	0.995

Nore: A is the pre-exponential factor, *R* is the universal gas constant.

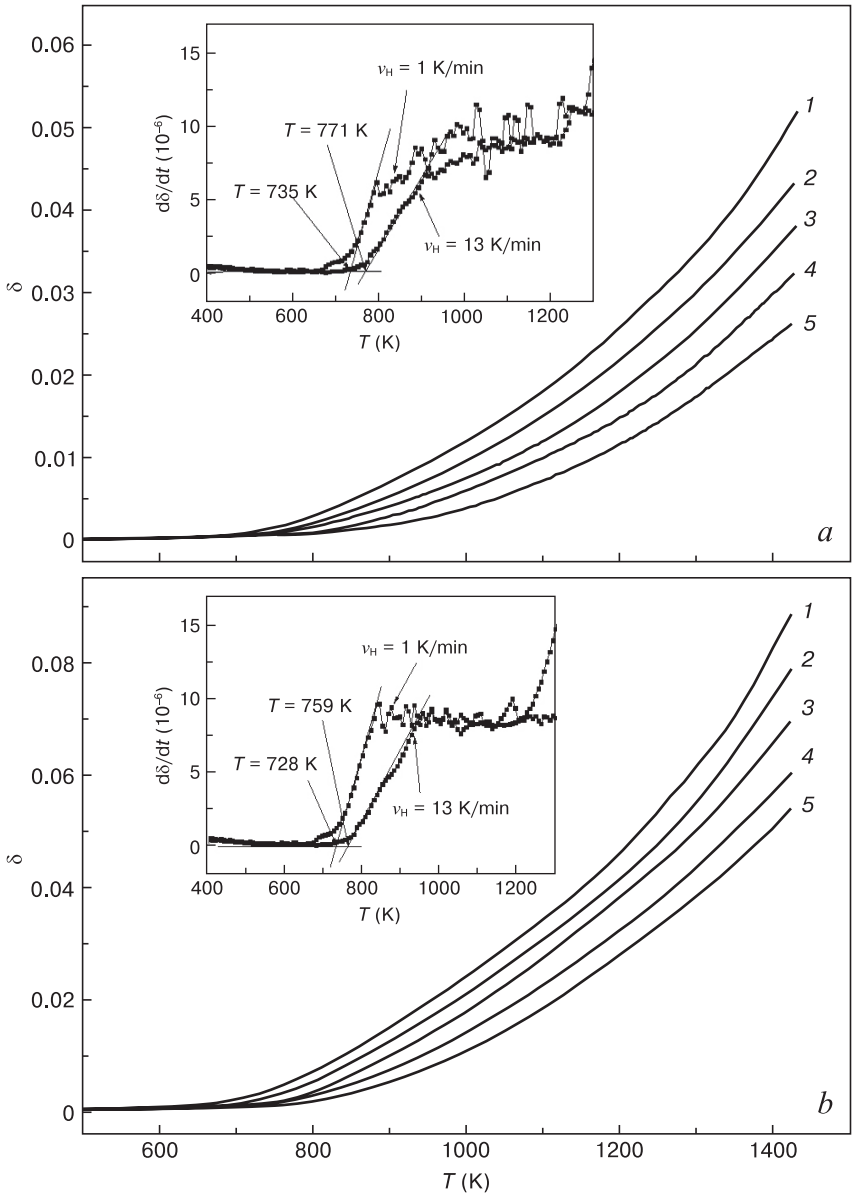

Figure 4. Temperature dependence of the oxygen nonstoichiometry of $La_{0.7}Sr_{0.3}Mn_{0.9}Fe_{0.1}O_{3-\delta}$ samples at pO_2 = 400 Pa (*a*) and pO_2 = 10 Pa (*b*) with different heating rates (1 deg/min (*1*), 4 deg/ min (*2*), 7 deg/min (*3*), 10 deg/min (*4*), 13 deg/min (*5*))

difference between these models is based on the limited rate of chemical reactions [22–26]. In solid phase reactions, the reactants do not mix at the atomic level and, therefore, must diffuse into the reaction zone or mutually penetrate into each other. There are two fundamental chemical processes that determine the course of solid-state reactions: (a) the chemical reaction itself and (b) the transfer of a substance to the reaction zone. Usually, for each of them there is a certain activation energy (E_a), since each reaction implies a certain rate constant of oxygen evolution [22–27]. In this work, we will establish the value of the activation energy for oxygen desorption, which takes into account two processes: oxygen diffusion to the grain surface and a chemical reaction at the gas-solid interface.

The calculation of the activation energy of oxygen desorption was carried out by the Merzhanov method based on TGA data obtained under dynamic heating conditions at a constant rate of temperature increase from the basic equation of first-order chemical reaction kinetics [22–23]:

$$d\delta/dt = kf(\delta), \quad (3)$$

where $d\delta/dt$ is the oxygen desorption rate, k is the rate constant of the reaction and oxygen evolution, and $f(\delta)$ is an analytical function that depends on the reaction mechanism, t is the oxygen desorption process time. In this case, the rate constant of the oxygen evolution reaction can be expressed through the Arrhenius equation as follows [26]:

$$k = A\exp\left(-\frac{E_a}{RT}\right), \quad (4)$$

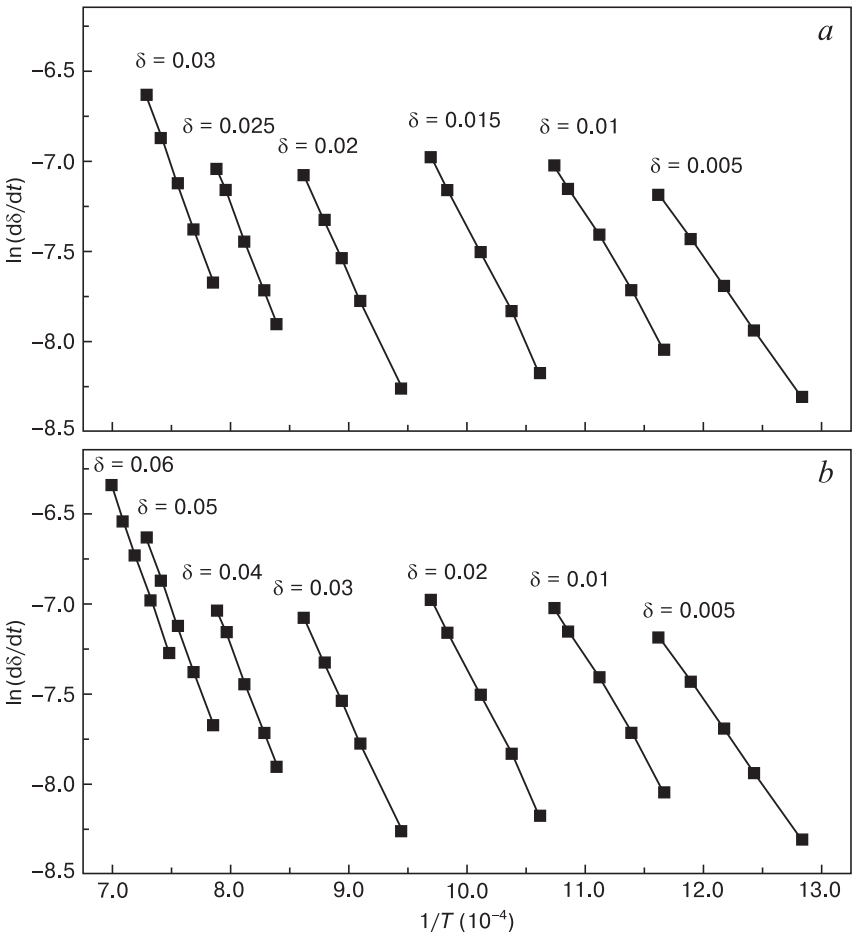

Figure 5. Dependence $\ln(d\delta/dt)_v - f(1/T)$ for different values of the oxygen index of samples $La_{0.7}Sr_{0.3}Mn_{0.9}Fe_{0.1}O_{3-\delta}$ at pO_2 = 400 Pa (*a*) and pO_2 = 10 Pa (*b*)

where A is the pre-exponential factor, R is the universal gas constant and T is the absolute temperature. Using expression (4), the kinetic equation (3) can be written as:

$$\ln\left[\frac{d\delta}{dt}\right] = \ln\left[Af(\delta)\right] + \left(-\frac{E_a}{RT}\right), \quad (5)$$

The activation energy can be determined by plotting the dependence of $\ln[d\delta/dt]$ on $1/T$ at different heating rates 1, 4, 7, 10 and 13 deg/min, which will allow us to estimate the effect of oxygen nonstoichiometry δ on the value of E_a. In this regard, based on the experimental dependences $\delta = f(T)$, the temperatures corresponding to the achievement of the same values of oxygen nonstoichiometry at different heating rates were determined. Then, for the established set of temperatures at fixed values of δ, pO_2 = 400 Pa and pO_2 = 10 Pa, dependences $\ln(d\delta/dt)_v - f(1/T)$ were plotted and E_a was calculated from the slopes of the lines, according to the formula:

$$E_a = -R\left[d\ln\left(\frac{d\delta}{dt}\right)_v \Big/ d\left(\frac{1}{T}\right)\right], \quad (6)$$

where t is the duration of the process, R is the universal gas constant, T is the temperature of the experiment (Fig. 5). If only one oxygen diffusion mechanism dominates during the reaction, then the lines will be parallel. Otherwise, there will be several diffusion mechanisms.

It has been established that for the $La_{0.7}Sr_{0.3}Mn_{0.9}Fe_{0.1}O_{3-\delta}$ sample, the slope of the straight lines $\ln(d\delta/dt)_v - f(1/T)$ decreases monotonically with increasing δ, indicating

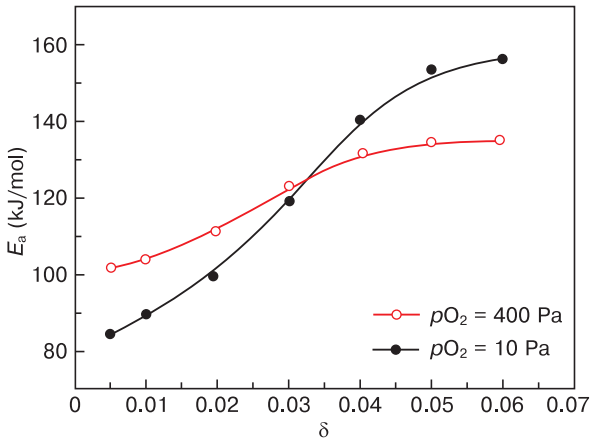

Figure 6. Dependences of the activation energy of oxygen diffusion E_a on the oxygen index in samples $La_{0.7}Sr_{0.3}Mn_{0.9}Fe_{0.1}O_{3-\delta}$ at pO_2 = 400 Pa and pO_2 = 10 Pa

that the activation energy depends on the concentration of oxygen vacancies. Thus, at the initial stage of oxygen evolution from $La_{0.7}Sr_{0.3}Mn_{0.9}Fe_{0.1}O_{3-\delta}$ at pO_2 = 400 Pa, the oxygen desorption activation energy has a minimum value E_a = 103.7 kJ/mol at δ = 0.005 and as the concentration of oxygen vacancies increases it increases with reaching saturation at E_a = 134.3 kJ/mol and δ = 0.06 (Fig. 6). Reducing the partial pressure of oxygen to pO_2 = 10 Pa increases the activation energy of oxygen diffusion to E_a = 158.8 kJ/mol at δ = 0.06 (Fig. 6). It is quite possible that as the concentration of oxygen vacancies $(V_O)^{\bullet\bullet}$ increases, they interact with subsequent processes of their ordering with the formation of associates. In this case, anion vacancies contribute to the redistribution of the electron density and the transition of some of the iron cations to the lower spin states $Fe^{3+} + e^- \rightarrow Fe^{2+}$ and $Mn^{3+} + e^- \rightarrow Mn^{2+}$.

4. Conclusion

According to the temperature dependences of TGA performed at various partial pressures of oxygen (400 Pa and 10 Pa), it was found that the value of the oxygen index δ for the $La_{0.7}Sr_{0.3}Mn_{0.9}Fe_{0.1}O_{3-\delta}$ compound increases with rising temperature equidistantly for all heating rates and does not reach saturation up to T = 1400 K, above which decomposition of the compound starts.

The calculation of the activation energy of oxygen desorption by the Merzhanov method at different oxygen partial pressure values (from pO_2 = 400 Pa to pO_2 = 10 Pa) showed that on the initial stage of oxygen release from $La_{0.7}Sr_{0.3}Mn_{0.9}Fe_{0.1}O_{3-\delta}$, the activation energy of oxygen desorption has a minimum value and, as the concentration of oxygen vacancies increases, it rises with reaching saturation.

It is supposed that as the concentration of oxygen vacancies $(V_O)^{\bullet\bullet}$ increases, they interact with subsequent processes of their ordering with the formation of associates. At the same time, anion vacancies contribute to the redistribution of the electron density and the transition of some of the iron and manganese cations to the lower spin states $Fe^{3+} + e^- \rightarrow Fe^{2+}$ and $Mn^{3+} + e^- \rightarrow Mn^{2+}$.

Acknowledgment

The authors are grateful for the support of this study within the framework of the BRFFR projects No. F21IZR-004 and No. F21U-003.

References

1. Goodenough J.B. Electronic and ionic transport properties and other physical aspects of perovskites. *Reports on Progress in Physics*. 2004; 67: 1915–1994. https://doi.org/10.1088/0034-4885/67/11/R01
2. Balagurov A.M., Bushmeleva S.N., Pomjakushin V.Yu., Sheptyakov D.V., Amelichev V.A., Gorbenko O.Yu., Kaul A.R., Gan'shina E.A., Perkins N.B. Magnetic structure of $NaMnO_3$ consistently doped with Sr and Ru. *Physical Review B*. 2004; 70: 014427. https://doi.org/10.1103/PhysRevB.70.014427
3. Dunaevsky S.M. Magnetic phase diagrams of manganites in the area of their electronic doping (a Review). *Fizika Tverdogo Tela*. 2004; 46(2): 193–211. (In Russ.)
4. Kozlenko D.P., Glazkov V.P., Jirák Z., Savenko B.N. High pressure effects on the crystal and magnetic structure of $Pr_{1-x}Sr_xMnO_3$ manganites (x = 0.5–0.56). *Journal of Physics: Condensed Matter*. 2004; 16(13): 2381–2394. https://doi. org/10.1088/0953-8984/16/13/017
5. Yanchevskii O.Z., V'yunov O.I., Belous A.G., Tovstolytkin A.I., Kravchik V.P. Synthesis and properties of $La_{0.7}Sr_{0.3}Mn_{1-x}Ti_xO_3$. *Fizika Tverdogo Tela*. 2006; 48(4): 667–673. (In Russ.)
6. McIntosh S., Vente J.F., Haije W.G., Blank D.H.A., Bouwmeester H.J.M. Structure and oxygen stoichiometry of $SrCo_{0.8}Fe_{0.2}O_{3-\delta}$ and $Ba_{0.5}Sr_{0.5}Co_{0.8}Fe_{0.2}O_{3-\delta}$. *Solid State Ionics*. 2006; 177(19–25): 1737–1742. https://doi.org/10.1016/j.ssi.2006.03.041
7. Nagaev E.L. Lanthanum manganites and other giant-magnetoresistance magnetic conductors. *Physics – Uspekhi*. 1996; 39(8): 781–806. https://doi.org/10.1070/PU1996v039n08ABEH000161
8. Maignan A., Martin C., Pelloquin D., Nguyen N., Raveau B. Structural and magnetic studies of ordered oxygen-deficient perovskites $LnBaCo_2O_{5+\delta}$, closely related to the "112" structure. *Journal of Solid State Chemistry*. 1999; 142(2): 247–260. https://doi.org/10.1006/jssc.1998.7934
9. Yamazoe N., Furukawa S., Teraoka Y., Seiyama T. The effect of oxygen sorption on the crystal structure of $La_{1-x}Sr_xCoO_{3-\delta}$. *Chemistry Letters*. 1982; 11(12): 2019–2022. https://doi.org/10.1246/cl.1982.2019
10. van den Brink J., Khaliullin G., Khomskii D. Charge and orbital order in half-doped manganites. *Physical Review Letters*. 1999; 83(24): 5118. https://doi.org/10.1103/PhysRevLett.83.5118
11. Deshmukh A.V., Patil S.I., Bhagat S.M., Sagdeo P.R., Choudhary R.J., Phase D.M. Effect of iron doping on electrical, electronic and magnetic properties of $La_{0.7}Sr_{0.3}MnO_3$. *Journal of Physics D: Applied Physics*. 2009; 42(18): 185410. https://doi.org/10.1088/0022-3727/42/18/185410
12. Kuo J.H., Anderson H.U., Sparlin D.M. Oxidation-reduction behavior of undoped and Sr-doped $LaMnO_3$: defect structure, electrical conductivity, and thermoelectric power. *Journal of Solid State Chemistry*. 1990; 87(1): 55–63. https://doi. org/10.1016/0022-4596(90)90064-5
13. Kruidhof H., Bouwmeester H.J.M., v. Doorn R.H.E., Burggraaf A.J. Influence of order-disorder transitions on oxygen permeability through selected nonstoichiometric perovskite-type oxides. *Solid State Ionics*. 1993; 63–65: 816–822. https://doi.org/10.1016/0167-2738(93)90202-E
14. Ritter C., Ibarra M.R., Morellon L., Blasco J., Garcia J., De Teresa J.M. Structural and magnetic properties of double perovskites

AA'FeMoO$_6$ (*AA*' = Ba$_2$, BaSr, Sr$_2$ and Ca$_2$). *Journal of Physics: Condensed Matter*. 2000; 12(38): 8295–8308. https://doi.org/10.1088/0953-8984/12/38/306

15. Goodenough J.B. Metallic oxides. *Progress in Solid State Chemistry*. 1971: 5: 145–399. https://doi.org/10.1016/0079-6786(71)90018-5
16. Troyanchuk I.O., Bushinsky M.V., Szymczak H., Bärner K., Maigna A. Magnetic interaction in Mg, Ti, Nb doped manganites. *European Physical Journal B*. 2002: 28(1): 75–80. https://doi.org/10.1140/epjb/e2002-00202-2
17. Ulyanov A.N., Mazur A.S., Yang D.C., Krivoruchko V.N., Danilenko I.A., Konstantinova T.E., Levchenko G.G. Local structural and magnetic inhomogeneities in nanosized $La_{0.7}Sr_{0.3}MnO_3$ manganites. *Nanosystems, Nanomaterials, Nanotechnologies*. 2011; 9(1): 107–114. (In Russ.)
18. Kalanda N.A., Yarmolich M.V., Gurskii A.L., Petrov A.V., Zhaludkevich A.L., Ignatenko O.V., Serdechnova M. Oxygen nonstoichiometry and magnetic properties of doped manganites $La_{0.7}Sr_{0.3}Mn_{0.95}Fe_{0.05}O_{3-\delta}$. *Izvestiya Vysshikh Uchebnykh Zavedenii. Materialy Elektronnoi Tekhniki = Materials of Electronics Engineering*. 2022; 25(1): 52–63. (In Russ.). https://doi.org/10.17073/1609-3577-2022-1-52-63
19. dos Santos-Gómez L., Leon-Reina L., Porras-Vazquez J.M., Losilla E.R., Marrero-Lopez D. Chemical stability and compatibility of double perovskite anode materials for SOFCs. *Solid State Ionics*. 2013; 239: 1–7. https://doi.org/10.1016/j.ssi.2013.03.005
20. Kraus W. POWDER CELL – a program for the representation and manipulation of crystal structures and calculation of the resulting X-ray powder patterns. *Journal of Applied Crystallography*. 1996; 29(3): 301–303. https://doi. org/10.1107/S0021889895014920
21. Rodríguez-Carvajal J. Recent developments of the program FULLPROF. Commission on powder diffraction (IUCr). *Newsletter*. 2001; 26: 12–19.
22. Merzhanov A.G., Barzykin V.V., Shteinberg A.S., Gontkovskaya V.T. Methodological Principles in studying chemical reaction kinetics under conditions of programmed heating. *Thermochimica Acta*. 1977; 21(3): 301–332. https://doi.org/10.1016/0040-6031(77)85001-6
23. Sánchez-Rodríguez D., Eloussifi H., Farjas J., Roura P., Dammak M. Thermal gradients in thermal analysis experiments: Criterions to prevent inaccuracies when determining sample temperature and kinetic parameters. *Thermochimica Acta*. 2014; 589: 37–46. https://doi.org/10.1016/j.tca.2014.05.001
24. Kalanda N.A. Thermally stimulated oxygen desorption in $Sr_2FeMoO_{6-\delta}$. *Izvestiya Vysshikh Uchebnykh Zavedenii. Materialy Elektronnoi Tekhniki = Materials of Electronics Engineering*. 2018; 21(1): 48–53. (In Russ.). https://doi.org/10.17073/1609-3577-2018-1-48-53
25. Tretyakov Yu.D. Development of inorganic chemistry as a fundamental basis for the creation of new generations of functional materials. *Uspekhi Khimii.* 2004: 73(9): 899–916. (In Russ.)
26. Stiller V. Arrhenius equation and non-equilibrium kinetics. VCH Pub. 1989. 176 p.
27. Mizusaki J., Mori N., Takai H., Yonemura Y., Minamiue H., Tagawa H., Dokiya M., Inaba H., Naraya K., Sasamoto T., Hashimoto T. Oxygen nonstoichiometry and defect equilibrium in the perovskite-type oxides $La_{1-x}Sr_xMnO_{3+d}$. *Solid State Ionics*. 2000; 129(1-4): 163–177. https://doi.org/10.1016/S0167-2738(99)00323-9